Extracellular Vesicle-delivered Bone Morphogenetic Proteins: A novel paracrine mechanism during embryonic development

Thomas Draebing[1, 2], Jana Heigwer[1, 2], Lonny Juergensen[1], Hugo Albert Katus[1, 2], David Hassel[1,2] *

[1] Department of Internal Medicine III, University Hospital Heidelberg, 69120 Heidelberg, Germany

[2] DZHK (German Centre for Cardiovascular Research), Partner Site Heidelberg/Mannheim, 69120 Heidelberg, Germany.

* Correspondence: david.hassel@gmail.com

Morphogens including Wnt, Hedgehog and BMP proteins are essential during embryonic development and early induction of organ progenitors. Besides free diffusion to form signalling gradients, extracellular vesicle- (EV-) mediated morphogen transport was identified as a central mechanism for Wnt- and Hh-signalling. Here, we investigated EVs isolated from whole zebrafish embryos as a potential morphogen transport mechanism. Inhibition of EV-secretion during development leads to severe dorsalization phenotypes, reminiscent of disrupted BMP-signalling. Subsequently, we found that EVs isolated

from zebrafish embryos at bud stage contain biologically active BMP2/4 protein. Embryos with inhibited EV secretion display reduced Smad1/5/9-phosphorylation and downstream gene expression activity. We further show that BMP-containing EVs are secreted by endodermal cells *in vitro*, and inhibition of endodermal-EV release *in vivo* causes signs of BMP signalling loss. Our data provides evidence that establishes the transport of BMP2/4 by EVs as an essential but so far undiscovered mechanism in developmental morphogenesis.

Introduction

During embryogenesis, a diverse set of cells originates from a single cell of origin. A major task during development is to ensure the correct position and fate of cells. The initially seemingly identical cells start to express a specific set of genes, thereby differentiating into new cell types. This process follows a specific pattern and requires intensive regulation and communication between cells and tissues[1]. Molecules mediating tissue patterning are called morphogens. A hallmark of morphogens is to form a gradient[2] and to thereby activate concentration dependent signalling responses[3, 4].

The formation of morphogen gradients is facilitated by multiple components and mechanisms, which are still not fully understood. Extracellular morphogens are typically thought to be secreted into the extracellular space as freely diffusing, unpackaged proteins[5, 6]. First models described the gradient formation by diffusion

and uptake of morphogens by cells either at the end ('source-sink' model[7]) or along the gradient ('synthesis-diffusion-degradation' model[7, 8]). More recent findings added more complexity to the existing models. Several soluble and membrane-bound proteins were found to bind morphogens. Depending on the binding factor and context the binding can lead to opposing effects. Thus, binding of bone morphogenetic proteins (BMPs) to Chordin inhibits receptor binding[9, 10], but can also facilitate increased diffusion rates[11]. BMPs also bind to plasma membrane-bound heparan sulphate proteoglycans (HSPGs), which removes the ability to diffuse freely[12, 13]. Knockout of HSPGs however also disrupts BMP-signalling[12, 13].

Recently, the morphogens Wnt, TGF-β and Hedgehog have been reported to reside in extracellular vesicles (EVs)[14-17]. The term EV describes a superfamily of vesicles that are characterized by their secretion from cells[18]. EVs include microvesicles (MV) and exosomes among other subtypes. Currently the different types of EVs are mainly characterized by their size, content and cellular compartment, in which they are synthesized. MVs are between 100 - 1.000 nm in size and are formed and shed at the plasma membrane of the secreting cell[19, 20]. Exosomes are the smallest kind of vesicles with a diameter of 50-150 nm in size[19, 20]. They form inside multivesicular bodies (MVBs), a part of the endosomal pathway, which can fuse with the plasma membrane, thereby releasing the exosomes[21]. The increasing attention EVs received during recent years is mostly due to their function in transporting specific sets of multiple biomolecules to target cells over long distances[22-25]. The transport of multiple molecules by the same vehicle allows the reliable delivery of complex and fine-tuned signals, while packaging of signalling molecules inside EVs might protect them from

66 degradation and antagonists. Investigating the role of EVs in morphogenetic signalling
67 may thus reveal an additional way of fine tuning morphogenesis during development.
68 Here we report that BMP2 and/or BMP4 (BMP2/4) are secreted in exosome-like EVs
69 *in vitro* and *in vivo* during embryogenesis. This EV-associated BMP was functionally
70 active and activated BMP-dependent transcription in cells. Inhibiting EV-release
71 strongly disturbed BMP-signalling in zebrafish, leading to phenotypes similar to the
72 phenotypes caused by dorsomorphin, a BMP inhibitor. We postulate that EV-
73 association of BMP is an additional tool to shape the BMP gradient.
74

75 ## Results

76 **Zebrafish secrete EVs during development**

77 To investigate the role of EVs during embryonic development, we chose the zebrafish
78 as a well-established model in developmental research[26]. EV isolation protocols
79 established so far are mostly optimized to purify EVs from bioliquids, like blood plasma
80 or cell culture media, while only limited options exist for purifying EVs from solid
81 tissue[27, 28]. We adapted existing EV isolation procedures to establish a protocol that
82 allowed us an enzyme-free isolation of EVs from early-stage zebrafish embryos by
83 using EDTA and mild shear forces to dissociate embryonic cells, thereby freeing EVs
84 (Figure 1A). EVs were then isolated by sequential ultracentrifugation[14, 28].
85 Nanoparticle tracking analysis (NTA) demonstrated an enrichment of particles with a
86 mode size of 140.3 nm in the isolates, which is within the size range of exosomes
87 (Figure 1B). Electron microscopy showed vesicles of smaller than 200 nm in size,

presenting the typical cup-like shape as previously described for EVs[28] (Figure 1C). Western blot analysis additionally showed the presence of the EV-proteins TSG101, Lamp1 and ALIX in both cell lysate and EV isolates, while the endoplasmic reticulum (ER)-marker GP96 was only present in cell lysate, but not in EVs (Figure 1D). This data indicates a pure EV-isolate with strong enrichment of exosome-like particles secreted by zebrafish embryos.

Inhibition of EV-secretion in zebrafish embryos causes a phenotype resembling dysfunctional BMP-signalling

To evaluate the relevance of EVs during embryonic development, we inhibited EV-secretion by morpholino-based knock down of Rab11a and Rab35. Rab11a and Rab35 are known to be essential for fusion of the multi vesicular body (MVB) with the plasma membrane and therefore are well-established molecular targets to block EV-release into the interstitium[29-31]. To validate the inhibition of EV secretion, EVs were isolated from 130 control- or morphant embryos and compared on the basis of the amount of ALIX present in the samples as determined by western blotting (Figure 2A). EV-isolates of Rab11a-morphants (125 µM MO-Rab11a) showed a non-significant reduction in ALIX content (-14.3 ± 20.7 %) (mean ± standard deviation). Rab35-morphants (250 µM MO-Rab35) however presented a significant reduction of 49.2 ± 29.2 % and were used in further experiments (Figure 2B). The knockdown (KD) of Rab35 resulted in a dorsalization phenotype with varying penetrance and severity (Figure 2C). Classifying phenotype severity using the dorsalization categories published by Mullins et al.[32] indicated that 34.0 % of the morphants presented severe dorsalization (C4-5), 8.2 %

with weak dorsalization (C1-3) and 27.8 % were dead, while only 29.9 % presented no dorsalization phenotype (Figure 2C). Dorsalization is a typical sign of dysfunctional morphogen signalling during dorso-ventral-patterning, especially of reduced BMP2, BMP4 or BMP7-signalling activity[33-36]. Inhibition of BMP signalling by dorsomorphin during embryonic development resulted in an identical phenotype (Figure 2C).

EVs in zebrafish embryos at bud stage contain BMPs

To assess whether BMPs are transported by embryonic zebrafish EVs, we performed western blotting of zebrafish EVs secreted at bud stage (10 hpf). The antibody was chosen to recognize the mature domain of BMP2, allowing the detection of both processed and unprocessed BMP2. Since the mature domain of BMP2 and BMP4 are nearly identical, the antibody detected both BMPs. Thus, we will refer to the detected BMPs as BMP2 and/or BMP4 (BMP2/4). Surprisingly, we detected the BMP2/4-precursor as well as the mature BMP2/4 ligand (Figure 2D). To confirm that BMP2/4 is associated to EVs and not purified as a contaminant, the crude EV-suspension was separated on an OptiPrep®-gradient (Figure 2E). BMP2/4 mainly co-purified within the same fractions as TSG101 at a density of 1.13 - 1.18 g/mL, which was previously described for EVs[19, 28]. In Rab35-morphants the amount of BMP2/4 in EV-isolates was significantly reduced as compared to EV-isolates obtained from control zebrafish, while BMP2/4-levels remained constant in the cell lysate of the same embryos (Figure 2F,G). Rab11-KD on the other hand did not reduce the amount of BMP2/4 in EV-isolates.

To demonstrate the biological activity of EV-associated BMP, we performed a dual luciferase reporter assay in HEK293A cells using a construct expressing Firefly

Luciferase under the control of BMP-responsive elements (BRE)[37]. Since zebrafish EVs might not actually be endocytosed by HEK293A-cells, we verified the uptake by labelling the EVs using PKH26 and imaged EV-treated cells after 5 h (Figure 2H). The cells showed a large number of fluorescent punctae, resembling endosomes, inside their cytosol, thereby indicating EV uptake. HEK293A cells were transfected with pGL3-BRE:Luciferase and pIS2-Renilla and subjected to a 16 h-treatment with either PBS or EVs isolated from zebrafish at bud stage. The EV-treatment resulted in a significant, dose-dependent increase in luciferase activity indicating that EV-delivered BMP indeed is able to activate BMP-dependent transcription (Figure 2I).

EV-transport of BMP2/4 is required for BMP-signalling during development

To address the hypothesis that BMP signalling is reduced by inhibition of EV-secretion, we used Nkx2.5, a transcriptional target of BMP2/4, as a readout to measure BMP-activated transcriptional activity in Rab35-morphants. Whole mount *in situ* hybridisation (WISH)-stainings of *nkx2.5* at the 7-somite stage (7SS) resulted in a typical staining with two parallel stripes along the midline, representing cardiac progenitor cells, in wildtype zebrafish embryos and control morphants[38] (Figure 3A). In Rab35-morphants we found the *nkx2.5*-positive areas to be smaller and situated more laterally (Figure 3A). Quantification of the *nkx2.5*-staining showed a significant reduction of the *nkx2.5*-expression to a median of 36.9 % (Quantiles (25 % - 75 %): 12.4 – 87.8 %) in Rab35-morphants as compared to wildtype zebrafish embryos. These results suggested that inhibition of EV-secretion results in reduced BMP-mediated transcriptional activity.

A well-observable and strong BMP-signalling event during early zebrafish development happens in the tail bud during tail development[39]. We used whole mount immunofluorescence stainings to detect phosphorylated Smad1/5/9 (pSmad1/5/9) in the tail bud of 7SS zebrafish embryos as an additional measure of BMP-signalling activity (Figure 3C). Again, while levels of pSmad1/5/9 were indistinguishable in wildtype and MO-Cntr-injected zebrafish, Rab35-KD significantly reduced the overall Smad1/5/9-phosphorylation in the tail bud to 45.4 % (Quantiles (25 % - 75 %): 28.4 – 77.0 %) (Figure 3D).

Taken together, these experiments strongly suggest that EVs play a crucial role in mediating BMP signalling activity and that EV-mediated BMP signalling is significantly involved in early cardiac progenitor cell induction.

Endoderm cells secrete EVs containing BMP2/4

BMP2 responsible for activating the transcription of Nkx2.5 in cardiac mesoderm cells is known to originate from the endoderm[40-42]. Since the EV isolation protocol for zebrafish embryos does not allow purification of EVs originating from a specific tissue or cell type, we used the mouse endodermal cell line End2 as an endodermal *in vitro* model [43]. Using western blotting, we verified the purity of the End2-EVs purified from cell culture medium (Figure 4A). Western blotting also confirmed that BMP2/4 was present in EVs isolated from End2-cells. The purity of End2-EV isolates was further asserted by electron microscopy (Figure 4B) and NTA measurements (Figure 4C), confirming an enrichment of particles smaller than 200 nm with a mode diameter of 140.6 nm. On an OptiPrep®-gradient BMP2/4 largely co-purified in the same fractions as the EV-markers Flot1 and ALIX, suggesting their association (Figure 4D).

PKH26-labeling again confirmed the uptake of End2-derived EVs by HEK293A-cells (Figure 4E), providing the basis for dual luciferase assays to test BMP-activity. As expected, the BMP-activity assay verified the ability of End2-EVs to activate BMP-dependent transcription (Figure 4F). Further, fluorescently labelled BMP2 (Venus-BMP2) expressed in End2-cells was detected in EV-isolates. After treatment of HEK293A-cells with PKH26-labelled EVs from Venus-BMP2-expressing End2-cells, overlapping fluorescent signals for PKH26 and Venus were found in the HEK293A-cells, again confirming EV and BMP 2/4 association (Figure 4G).

Endoderm-specific inhibition of EV-secretion dampens Smad1/5/9-phosphorylation in the zebrafish tail bud *in vivo*

To assess the significance of the endoderm as a source of EV-associated BMP2/4 *in vivo* we injected zebrafish embryos with a plasmid construct expressing a dominant negative variant of Rab35 ($Rab35^{N120I}$)[29] tagged with an N-terminal GFP ($GFP\text{-}Rab35^{dn}$). An endoderm-specific expression was achieved by using the *sox17*-promoter[44]. Since zebrafish stably expressing $GFP\text{-}Rab35^{dn}$ were not viable, transient expression was used instead, leading to a mosaic expression pattern only. Nevertheless, the expression of $Rab35^{dn}$ in the endoderm resulted in a similar phenotype as the ubiquitous Rab35-KD (Figure 5A, S1A), indicating that the endoderm is an important source for EVs involved in BMP-signalling. Surprisingly, overexpressing the wildtype form of Rab35 in the endoderm also increased the mortality and number of dorsalized embryos, although to a lesser extent than $Rab35^{dn}$.

Immune fluorescence stainings against pSmad1/5/9 showed that the expression of $GFP\text{-}Rab35^{dn}$ in contrast to expression of GFP or GFP-Rab35 resulted in morphological

changes and reduced fluorescence in the tail bud (Figure 5B). Quantification of the pSmad1/5/9 distribution and intensity in the tail bud validated these initial observations (Figure 5C). Interestingly, no overlap of the transgene-expressing cells with cells positive for pSmad1/5/9 was needed to cause the observed phenotype, indicating that a paracrine effect might be the cause for the reduced Smad1/5/9-phosphorylation (Figure S1C). Thus, our results suggest that endoderm-derived EVs are required for BMP-signalling during zebrafish development.

BMP2/4 is tethered to EV surfaces by binding to HSPGs

BMPs, other than Wnts or Hh, do not possess a lipid anchor, with which they can bind to EV-membranes[45-47]. However, BMPs are known to bind to heparan sulphate proteoglycans (HSPGs) on cell surfaces[13, 48, 49]. Since HSPGs are present on EV-surfaces as well[50], we investigated whether BMPs are tethered to EVs by HSPGs. We divided End2-EV isolates into two equal fractions. Fraction I was treated with Heparinase 3, which cleaves off the sugar chains of HSPGs to which BMPs are bound[51]. Fraction II was used as a control. If HSPGs are present and are responsible in linking BMPs to EVs, Heparinase 3 treatment should result in the decrease in BMP signal using western blot. Heparinase 3-treatment indeed led to a decrease in BMP2/4 in the EV-isolate (Figure 6A,B), indicating that BMP2/4 is tethered to the EV surface in part by binding to HSPGs.

Discussion

Here, we report that BMP2 and/or BMP4 are transported by EVs during zebrafish development, a mechanism that was essential for BMP-dependent morphogenetic signalling during zebrafish development. We further provide a mechanism of tethering morphogens without lipid-modification to EVs.

Morphogenetic signalling has been investigated for over a century and while it is commonly accepted that diffusion gradients are a hallmark feature of morphogen signalling, the mechanisms behind the formation of morphogen gradients are still not definitely resolved[8, 52]. Differences in morphogen gradient formation do not only occur between different morphogens, but also between morphogenetic signalling events facilitated by the same morphogen. The Dpp-gradient during the dorso-ventral-patterning in drosophila, for example, is formed within 30 min by an active shuttling mechanism involving Sog[53, 54]. In the imaginal wing disc on the other hand, the Dpp-gradient needs 4 h to form, which is thought to happen by a different unaided mechanism[55]. Several additional models were proposed based on experimental observations. This includes the Source-Sink-model[7, 56, 57], the Counter-Gradient-model[56-58], restricted diffusion[11, 12], transcytosis[59], cytoneme transport[60] and more recently also vesicular transport[14-16, 61]. This role of EVs in morphogenetic signalling is by now a well-established mechanism after Wnt-proteins and Hh were found in EVs, a mechanism that allows these lipid-modified proteins to diffuse efficiently without unspecifically binding to membranes [14-16]. The observation that BMPs, that do not possess a lipid anchor, are transported by EVs as well, indicates that masking lipid groups is not the only function of EVs in morphogenetic signalling. EVs might be

needed to mobilize BMP that is bound to HSPGs on cell surfaces and thus restricted in their diffusion.

Multiple proteomics studies detected BMP in EVs but did not investigate this finding in detail[62-69]. Furthermore, the secretion of BMPs in matrix vesicles, a specialized type of EV that is involved in bone formation was reported earlier by Nahar et al.[61], further supporting our findings.

The phenotypical changes observed in zebrafish embryos after Rab35-KD suggest that EV-transport is essential for BMP-signalling during embryonic development. The severity of the phenotypes is surprising, considering that BMP is thought to diffuse unaided. But whether the importance of EVs in BMP-signalling is due to their ability to mobilize BMPs or due to other reasons, remains to be investigated. A limitation of this study is that known factors involved in EV-secretion, that can be manipulated to inhibit the release of EVs, are also involved in essential cellular processes, especially endosomal trafficking, including receptor recycling[29, 70, 71]. Thus, unspecific effects of changes in Rab35-activity might add to the observed phenotype. Our experiments however show that inhibition of Rab35 in the endoderm affected BMP-signalling activity in cells of the zebrafish tailbud, which are mesoderm cells[72]. Processes that take part in computing the BMP-signal response in the mesodermal target cells, as for example BMP-receptor recycling, cannot be influenced by Rab35^{dn} directly, that is exclusively expressed in the endoderm. This indicates, that a paracrine effect is likely responsible for the reduced Smad1/5/9-phosphorylation.

The finding, that EV-associated BMP2/4 is secreted by the endoderm, is intuitive, since the endoderm was already described to be responsible for secreting freely diffusing

268 BMP2/4 during early development[40-42]. Nevertheless, since BMP2/4 associate to EVs
269 by binding to HSPGs on their surface should theoretically be able to catch free BMP2/4
270 in the extracellular space. This would mean that EVs from cells, which are not secreting
271 BMP2/4, could be able to influence BMP2/4-signaling by secreting BMP-tethering EVs,
272 thereby modulating BMP gradient formation and thus BMP signalling. Whether this
273 hypothesis is true, remains to be investigated in future studies.
274 In summary, we describe an additional mode of transport for BMPs during embryonic
275 development. While future studies will have to show how EV-associated BMPs
276 contribute to BMP-signalling as compared to previously known mechanisms, the
277 findings presented here provide additional information, that will help to understand
278 the formation of BMP-gradients.
279

Experimental Procedures

Zebrafish care and maintenance

All animal experiments have been performed in accordance with the guidelines of the state of Baden-Wuerttemberg and all experimental protocols. Wildtype zebrafish were used as basis for all experiments. For imaging, zebrafish embryos were mounted in 2% methyl-cellulose and analysed under the microscope.

Inhibition of EV secretion

Morpholinos were obtained from Gene Tools LLC. The morpholinos against Rab11 and Rab35 were designed to bind at the translation start site. The sequences were as follows: Rab11[73]: 5'-GTATTCGTCGTCTCGTGTCCCCATC-3'; Rab35[74]: 5'-AGAGGTGATCGTAGTCGCGGGCCAT-3'. MO-Cntr: non-targeting standard control (Gene Tools LLC). Morpholinos were solubilized in water at a stock-concentration of 1 mM. Stock solutions were diluted with 200 mM KCl to working concentrations of 125 µM–250 µM. The injection volume was 2 – 4 nL/embryo. Effective doses were determined for every morpholino separately.

Inhibition of EV secretion was verified by western blot analysis using an antibody targeting ALIX (see below). EVs of uninjected and MO-Cntr-injected zebrafish embryos were used as controls. Experiments showing large differences in ALIX-content of EVs between uninjected and MO-Cntr-injected zebrafish embryos were excluded.

Cell Culture

HEK293A-cells were maintained in Dulbecco's Modified Eagle Medium (DMEM) (Gibco) containing 10 % Foetal Calf Serum (FCS) (Gibco), 1 % L-Glutamine (Gibco) and 1 % Penicillin/Streptavidin (Gibco). End2 cells[43] were maintained in DMEM/F-12

303 medium (Gibco) containing 7.5 % FCS and 1 % Penicillin/Streptavidin. All cells were
304 cultured at 37 °C and 5 % CO_2 in a humid atmosphere. Transient transfections of
305 plasmids were performed using Lipofectamine 2000 (Invitrogen) following the
306 manufacturer's instructions.

307 **EV Purification of Cell Culture Medium**

308 Cells were grown to 70 % confluency. The medium was exchanged with fresh medium
309 containing FCS, that was depleted from EVs by centrifugation at 100,000 g for 18 h
310 and successively filtered through a 0.2 µm filter. After 24 h the conditioned medium
311 was collected and EVs were isolated by ultracentrifugation following the protocol
312 described by Gross et al.[14].

313 **Nanoparticle Tracking Analysis**

314 The EV pellet were resuspended in PBS. Particle counts and size distribution were
315 measured using a NanoSight LM10 (Malvern Instruments) equipped with a 405 nm
316 laser.

317 **Electron Microscopy**

318 EVs resuspended in PBS were prepared for electron microscopy following the protocol
319 described by Théry et al.[28]

320 **OptiPrep Gradient Centrifugation**

321 EV pellets were resuspended in 500 µL Homogenization Media (0.25 M sucrose, 10
322 mM Tris-HCL, (pH 7.4)). 40 %, 20 %, 10 % and 5 % OptiPrep/Homogenization Media
323 solutions were prepared. The gradient was created by layering 3 mL of the 40 %, 20 %
324 and 10 % OptiPrep solutions and 2.5 mL of the 5 % OptiPrep solution in order. The EV
325 sample was layered on top of the gradient. The gradients were ultracentrifuged at

100,000 g for 18 h at 4 °C. Fractions of 1 mL were collected beginning from the top of the gradient and diluted with PBS. EVs in each fraction were isolated by ultracentrifugation at 100,000 g for 3 h at 4 °C.

Imaging EV uptake

For labelling with PKH26 (Sigma Aldrich) the EV pellet was resuspended in 1 mL Diluent C. 2 µL of PKH26 was added and the samples were incubated for 30 min at room temperature. Afterwards the sample was diluted by adding 11 mL of PBS. The labelled EVs were collected by ultracentrifugation at 100,000 g for 3 h at 4 °C. The EV pellet was resuspended in PBS. Cells were treated with 50 ug/mL of PKH26-labelled EVs. Life-cell imaging was performed 5 h after treatment.

***In vitro* BMP activity assay**

HEK293A cells seeded in 96-well plates were transfected with 10 ng pIS2-Renilla Control Vector and 100 ng pGL3-BRE:Luciferase[37]. The medium was exchanged to serum-free medium 1 h before treatment. Cells were either treated with EVs or PBS. 16 h post treatment cells were analysed using the Dual Luciferase Reporter Assay system (Promega, Cat.-No. E1960) following the manufacturer's instructions. Renilla Luciferase activity was used to normalize Firefly Luciferase activity.

Whole mount in situ hybridization

The whole mount in situ hybridization was performed as previously described by Thisse et al.[75] The probes to detect nkx2.5 were generated using the primer pair 5'-CGGGACATACTGAACCTGGA-3', 5'-TCTCCCAGACACGGTTTACC-3'. Staining intensity was quantified using Fiji (ImageJ). Images were contrasted consistently in each experiment. Each stained area (both heart fields) was segmented manually. The area

of the staining was normalized to the total area of the embryo. The background intensity was measured close to the stained area and used for background subtraction. The *nkx2.5*-expression was defined as the product of the background-corrected mean staining intensity and the normalized staining area.

Whole mount immunofluorescence

Zebrafish embryos fixed in 4 % PFA were dehydrated with an ascending methanol series. Before staining, the embryos were rehydrated with a descending methanol series and permeabilized by incubation with ice cold acetone for 8 min at -20 °C. Embryos were blocked in PBS with 1 % Triton-X100, 2 % BSA, 10 % sheep serum and 1 % DMSO for 30 min before incubation with the primary antibody for at least 20 h at 4 °C. Incubation with the secondary antibody was performed overnight at 4 °C. The staining intensity in the tail bud of the embryos was analysed in the same way as the *nkx2.5*-whole mount *in situ* stainings.

Heparinase 3-treatment

EVs resuspended in PBS were divided into two equal parts of which one was treated with 2 mIU/mL Heparinase 3 in reaction buffer (20 mM TrisHCl, 0.1 mg/mL BSA, 4 mM $CaCl_2$ (pH 7.5)) and the other with reaction buffer for 3 h at 37 °C. EVs were isolated from samples by ultracentrifugation with 100,000 g for 3 h at 4 °C before further analysis.

Antibodies

For western blotting experiments the following antibodies were used: GP96 (CST, #2104), TSG101 (Sigma Aldrich, AV38773), ALIX (Sigma Aldrich, sab4200476), Flotillin-

1 (BD Biosciences, 610821), LAMP1 (Sigma Aldrich, sab3500285), beta-Actin (Sigma Aldrich, A5441), pSmad1/5/9 (CST, #13820) and BMP2/4 (RnD Systems, MAB1128).

Statistics

Statistical tests used for analysis are indicated in the respective figure captions. Significance levels are indicated as follows: ns: not significant; *: $p \leq 0.05$; **: $p \leq 0.01$; ***: $p \leq 0.001$. If not indicated otherwise error bars represent the standard deviation.

Acknowledgements

We thank Prof. Dr. Michael Boutros for allowing us to perform NTA-measurements at his lab, Ms. Hosser for taking the electron microscopy images, Prof. Dr. Mummery for providing us with the End2-cell line, Prof. Dr. Mikael Simons for sharing Rab35-constructs and Prof. Dr. De Robertis for the Venus-BMP2 construct.

Author Contributions

D.H. and T.D. designed the experiments and wrote the article. T.D., J.H. and L.J. performed the experiments. T.D. analysed the data. H.A.K. and D.H. provided the material, read and revised the article.

References

1. Perrimon, N., Pitsouli, C. & Shilo, B.Z. Signaling mechanisms controlling cell fate and embryonic patterning. *Cold Spring Harb Perspect Biol* **4**, a005975 (2012).
2. Child, C.M. (Chicago, Ill., The University of Chicago Press, 1941).
3. Wolpert, L. Positional information and the spatial pattern of cellular differentiation. *J Theor Biol* **25**, 1-47 (1969).
4. Wolpert, L. Positional information and pattern formation. *Curr Top Dev Biol* **6**, 183-224 (1971).
5. Lander, A.D., Nie, Q. & Wan, F.Y. Do morphogen gradients arise by diffusion? *Dev Cell* **2**, 785-796 (2002).
6. Mizutani, C.M. et al. Formation of the BMP activity gradient in the Drosophila embryo. *Dev Cell* **8**, 915-924 (2005).
7. Crick, F. Diffusion in embryogenesis. *Nature* **225**, 420-422 (1970).
8. Wartlick, O., Kicheva, A. & González-Gaitán, M. Morphogen gradient formation. *Cold Spring Harb Perspect Biol* **1**, a001255 (2009).
9. Piccolo, S., Sasai, Y., Lu, B. & De Robertis, E.M. Dorsoventral patterning in Xenopus: inhibition of ventral signals by direct binding of chordin to BMP-4. *Cell* **86**, 589-598 (1996).
10. Sasai, Y. et al. Xenopus chordin: a novel dorsalizing factor activated by organizer-specific homeobox genes. *Cell* **79**, 779-790 (1994).
11. Eldar, A. et al. Robustness of the BMP morphogen gradient in Drosophila embryonic patterning. *Nature* **419**, 304-308 (2002).

12. Belenkaya, T.Y. et al. Drosophila Dpp morphogen movement is independent of dynamin-mediated endocytosis but regulated by the glypican members of heparan sulfate proteoglycans. *Cell* **119**, 231-244 (2004).

13. Bornemann, D.J., Duncan, J.E., Staatz, W., Selleck, S. & Warrior, R. Abrogation of heparan sulfate synthesis in Drosophila disrupts the Wingless, Hedgehog and Decapentaplegic signaling pathways. *Development* **131**, 1927-1938 (2004).

14. Gross, J.C., Chaudhary, V., Bartscherer, K. & Boutros, M. Active Wnt proteins are secreted on exosomes. *Nat Cell Biol* **14**, 1036-1045 (2012).

15. Gradilla, A.C. et al. Exosomes as Hedgehog carriers in cytoneme-mediated transport and secretion. *Nat Commun* **5**, 5649 (2014).

16. Matusek, T. et al. The ESCRT machinery regulates the secretion and long-range activity of Hedgehog. *Nature* **516**, 99-103 (2014).

17. Webber, J., Steadman, R., Mason, M.D., Tabi, Z. & Clayton, A. Cancer exosomes trigger fibroblast to myofibroblast differentiation. *Cancer Res* **70**, 9621-9630 (2010).

18. Raposo, G. & Stoorvogel, W. Extracellular vesicles: exosomes, microvesicles, and friends. *J Cell Biol* **200**, 373-383 (2013).

19. Théry, C., Ostrowski, M. & Segura, E. Membrane vesicles as conveyors of immune responses. *Nat Rev Immunol* **9**, 581-593 (2009).

20. Whiteside, T.L. Tumor-Derived Exosomes and Their Role in Cancer Progression. *Adv Clin Chem* **74**, 103-141 (2016).

21. Kowal, J., Tkach, M. & Théry, C. Biogenesis and secretion of exosomes. *Curr Opin Cell Biol* **29**, 116-125 (2014).

22. de Jong, O.G. et al. Cellular stress conditions are reflected in the protein and RNA content of endothelial cell-derived exosomes. *J Extracell Vesicles* **1** (2012).

23. Yáñez-Mó, M. et al. Biological properties of extracellular vesicles and their physiological functions. *J Extracell Vesicles* **4**, 27066 (2015).

24. Haraszti, R.A. et al. High-resolution proteomic and lipidomic analysis of exosomes and microvesicles from different cell sources. *J Extracell Vesicles* **5**, 32570 (2016).

25. Caby, M.P., Lankar, D., Vincendeau-Scherrer, C., Raposo, G. & Bonnerot, C. Exosomal-like vesicles are present in human blood plasma. *Int Immunol* **17**, 879-887 (2005).

26. Dawid, I.B. Developmental biology of zebrafish. *Ann N Y Acad Sci* **1038**, 88-93 (2004).

27. Vella, L.J. et al. A rigorous method to enrich for exosomes from brain tissue. *J Extracell Vesicles* **6**, 1348885 (2017).

28. Thery, C., Amigorena, S., Raposo, G. & Clayton, A. Isolation and characterization of exosomes from cell culture supernatants and biological fluids. *Curr Protoc Cell Biol* **Chapter 3**, Unit 3 22 (2006).

29. Hsu, C. et al. Regulation of exosome secretion by Rab35 and its GTPase-activating proteins TBC1D10A-C. *J Cell Biol* **189**, 223-232 (2010).

30. Savina, A., Vidal, M. & Colombo, M.I. The exosome pathway in K562 cells is regulated by Rab11. *J Cell Sci* **115**, 2505-2515 (2002).

460 31. Savina, A., Fader, C.M., Damiani, M.T. & Colombo, M.I. Rab11 promotes
461 docking and fusion of multivesicular bodies in a calcium-dependent
462 manner. *Traffic* **6**, 131-143 (2005).
463 32. Mullins, M.C. et al. Genes establishing dorsoventral pattern formation in the
464 zebrafish embryo: the ventral specifying genes. *Development* **123**, 81-93
465 (1996).
466 33. Steinbeisser, H., Fainsod, A., Niehrs, C., Sasai, Y. & De Robertis, E.M. The role
467 of gsc and BMP-4 in dorsal-ventral patterning of the marginal zone in
468 Xenopus: a loss-of-function study using antisense RNA. *EMBO J* **14**, 5230-
469 5243 (1995).
470 34. Hawley, S.H. et al. Disruption of BMP signals in embryonic Xenopus
471 ectoderm leads to direct neural induction. *Genes Dev* **9**, 2923-2935 (1995).
472 35. Kishimoto, Y., Lee, K.H., Zon, L., Hammerschmidt, M. & Schulte-Merker, S.
473 The molecular nature of zebrafish swirl: BMP2 function is essential during
474 early dorsoventral patterning. *Development* **124**, 4457-4466 (1997).
475 36. Arkell, R. & Beddington, R.S. BMP-7 influences pattern and growth of the
476 developing hindbrain of mouse embryos. *Development* **124**, 1-12 (1997).
477 37. Korchynskyi, O. & ten Dijke, P. Identification and functional
478 characterization of distinct critically important bone morphogenetic
479 protein-specific response elements in the Id1 promoter. *J Biol Chem* **277**,
480 4883-4891 (2002).
481 38. Peterkin, T., Gibson, A. & Patient, R. GATA-6 maintains BMP-4 and Nkx2
482 expression during cardiomyocyte precursor maturation. *EMBO J* **22**, 4260-
483 4273 (2003).

39. Pyati, U.J., Webb, A.E. & Kimelman, D. Transgenic zebrafish reveal stage-specific roles for Bmp signaling in ventral and posterior mesoderm development. *Development* **132**, 2333-2343 (2005).

40. Nascone, N. & Mercola, M. An inductive role for the endoderm in Xenopus cardiogenesis. *Development* **121**, 515-523 (1995).

41. Schultheiss, T.M., Xydas, S. & Lassar, A.B. Induction of avian cardiac myogenesis by anterior endoderm. *Development* **121**, 4203-4214 (1995).

42. Lough, J. et al. Combined BMP-2 and FGF-4, but neither factor alone, induces cardiogenesis in non-precardiac embryonic mesoderm. *Dev Biol* **178**, 198-202 (1996).

43. Mummery, C.L., Feijen, A., van der Saag, P.T., van den Brink, C.E. & de Laat, S.W. Clonal variants of differentiated P19 embryonal carcinoma cells exhibit epidermal growth factor receptor kinase activity. *Dev Biol* **109**, 402-410 (1985).

44. Alexander, J. & Stainier, D.Y. A molecular pathway leading to endoderm formation in zebrafish. *Curr Biol* **9**, 1147-1157 (1999).

45. Willert, K. et al. Wnt proteins are lipid-modified and can act as stem cell growth factors. *Nature* **423**, 448-452 (2003).

46. Porter, J.A., Young, K.E. & Beachy, P.A. Cholesterol modification of hedgehog signaling proteins in animal development. *Science* **274**, 255-259 (1996).

47. Chamoun, Z. et al. Skinny hedgehog, an acyltransferase required for palmitoylation and activity of the hedgehog signal. *Science* **293**, 2080-2084 (2001).

48. Bornemann, D.J., Park, S., Phin, S. & Warrior, R. A translational block to HSPG synthesis permits BMP signaling in the early Drosophila embryo. *Development* **135**, 1039-1047 (2008).

49. O'Connell, M.P. et al. HSPG modulation of BMP signaling in fibrodysplasia ossificans progressiva cells. *J Cell Biochem* **102**, 1493-1503 (2007).

50. Christianson, H.C., Svensson, K.J., van Kuppevelt, T.H., Li, J.P. & Belting, M. Cancer cell exosomes depend on cell-surface heparan sulfate proteoglycans for their internalization and functional activity. *Proc Natl Acad Sci U S A* **110**, 17380-17385 (2013).

51. Lohse, D.L. & Linhardt, R.J. Purification and characterization of heparin lyases from Flavobacterium heparinum. *J Biol Chem* **267**, 24347-24355 (1992).

52. Bier, E. & De Robertis, E.M. EMBRYO DEVELOPMENT. BMP gradients: A paradigm for morphogen-mediated developmental patterning. *Science* **348**, aaa5838 (2015).

53. Francois, V., Solloway, M., O'Neill, J.W., Emery, J. & Bier, E. Dorsal-ventral patterning of the Drosophila embryo depends on a putative negative growth factor encoded by the short gastrulation gene. *Genes Dev* **8**, 2602-2616 (1994).

54. Shimmi, O., Umulis, D., Othmer, H. & O'Connor, M.B. Facilitated transport of a Dpp/Scw heterodimer by Sog/Tsg leads to robust patterning of the Drosophila blastoderm embryo. *Cell* **120**, 873-886 (2005).

55. Bollenbach, T. et al. Precision of the Dpp gradient. *Development* **135**, 1137-1146 (2008).

531 56. Pomreinke, A.P. et al. Dynamics of BMP signaling and distribution during
532 zebrafish dorsal-ventral patterning. *Elife* **6** (2017).
533 57. Zinski, J. et al. Systems biology derived source-sink mechanism of BMP
534 gradient formation. *Elife* **6** (2017).
535 58. Schwank, G. & Basler, K. Regulation of organ growth by morphogen
536 gradients. *Cold Spring Harb Perspect Biol* **2**, a001669 (2010).
537 59. González, F., Swales, L., Bejsovec, A., Skaer, H. & Martinez Arias, A. Secretion
538 and movement of wingless protein in the epidermis of the Drosophila
539 embryo. *Mech Dev* **35**, 43-54 (1991).
540 60. Hsiung, F., Ramirez-Weber, F.A., Iwaki, D.D. & Kornberg, T.B. Dependence
541 of Drosophila wing imaginal disc cytonemes on Decapentaplegic. *Nature*
542 **437**, 560-563 (2005).
543 61. Nahar, N.N., Missana, L.R., Garimella, R., Tague, S.E. & Anderson, H.C. Matrix
544 vesicles are carriers of bone morphogenetic proteins (BMPs), vascular
545 endothelial growth factor (VEGF), and noncollagenous matrix proteins. *J*
546 *Bone Miner Metab* **26**, 514-519 (2008).
547 62. Hong, B.S. et al. Colorectal cancer cell-derived microvesicles are enriched
548 in cell cycle-related mRNAs that promote proliferation of endothelial cells.
549 *BMC Genomics* **10**, 556 (2009).
550 63. Hurwitz, S.N. et al. Proteomic profiling of NCI-60 extracellular vesicles
551 uncovers common protein cargo and cancer type-specific biomarkers.
552 *Oncotarget* **7**, 86999-87015 (2016).
553 64. Xiao, Z. et al. Analysis of the extracellular matrix vesicle proteome in
554 mineralizing osteoblasts. *J Cell Physiol* **210**, 325-335 (2007).

555 65. Gonzalez-Begne, M. et al. Proteomic analysis of human parotid gland
556 exosomes by multidimensional protein identification technology
557 (MudPIT). *J Proteome Res* **8**, 1304-1314 (2009).
558 66. Skog, J. et al. Glioblastoma microvesicles transport RNA and proteins that
559 promote tumour growth and provide diagnostic biomarkers. *Nat Cell Biol*
560 **10**, 1470-1476 (2008).
561 67. Demory Beckler, M. et al. Proteomic analysis of exosomes from mutant
562 KRAS colon cancer cells identifies intercellular transfer of mutant KRAS.
563 *Mol Cell Proteomics* **12**, 343-355 (2013).
564 68. Bruno, S. et al. Mesenchymal stem cell-derived microvesicles protect
565 against acute tubular injury. *J Am Soc Nephrol* **20**, 1053-1067 (2009).
566 69. Fraser, K.B. et al. LRRK2 secretion in exosomes is regulated by 14-3-3. *Hum*
567 *Mol Genet* **22**, 4988-5000 (2013).
568 70. Kouranti, I., Sachse, M., Arouche, N., Goud, B. & Echard, A. Rab35 regulates
569 an endocytic recycling pathway essential for the terminal steps of
570 cytokinesis. *Curr Biol* **16**, 1719-1725 (2006).
571 71. Allaire, P.D. et al. Interplay between Rab35 and Arf6 controls cargo
572 recycling to coordinate cell adhesion and migration. *J Cell Sci* **126**, 722-731
573 (2013).
574 72. Esterberg, R., Delalande, J.M. & Fritz, A. Tailbud-derived Bmp4 drives
575 proliferation and inhibits maturation of zebrafish chordamesoderm.
576 *Development* **135**, 3891-3901 (2008).

577 73. Jopling, H.M. et al. Endosome-to-Plasma Membrane Recycling of VEGFR2
578 Receptor Tyrosine Kinase Regulates Endothelial Function and Blood Vessel
579 Formation. *Cells* **3**, 363-385 (2014).
580 74. Dantas de Cantos, I. (UMI Dissertation Publishing, 2004).
581 75. Thisse, C. & Thisse, B. High-resolution in situ hybridization to whole-mount
582 zebrafish embryos. *Nat Protoc* **3**, 59-69 (2008).
583

584 **Figures**

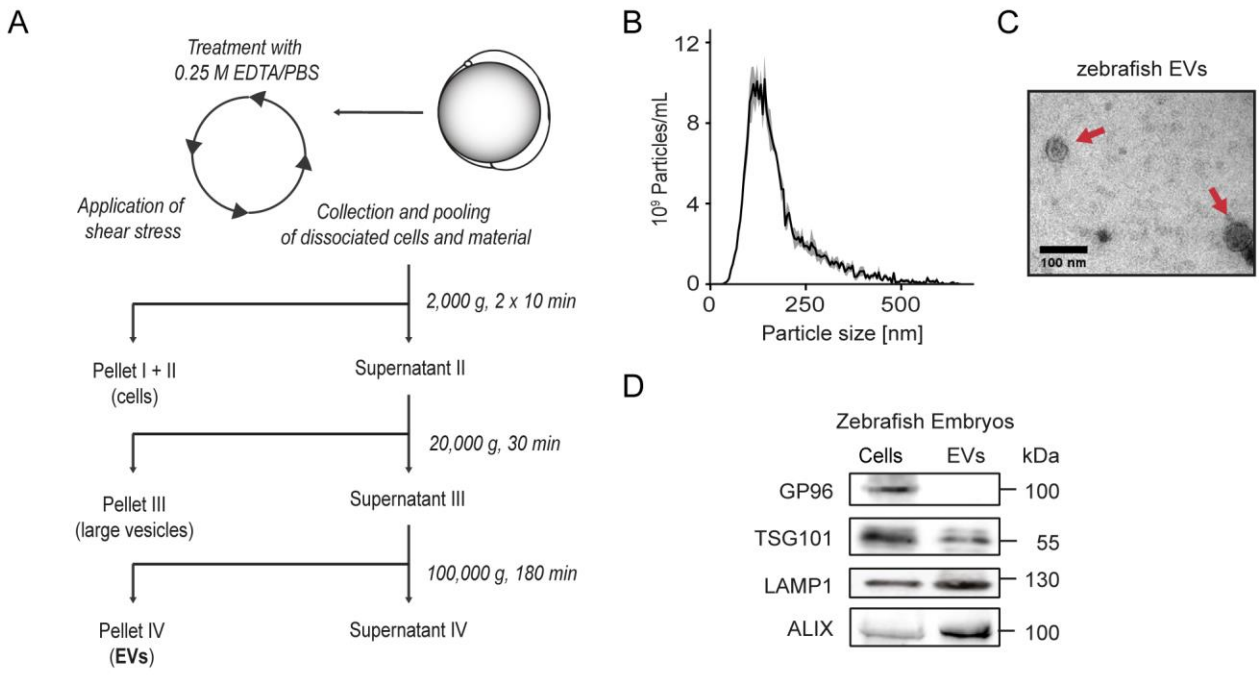

585 **Figure 1 | Isolation of EVs from zebrafish embryos.** (A) Schematic representation of
586 the protocol used to isolate EVs from zebrafish embryos. Experiments to verify the
587 purity of the EV-isolates were performed with EVs isolated from zebrafish embryos at
588 bud stage (10 hpf): (B) The particle size distribution in the EV-isolates was determined
589 by NTA measurements. The mean of five measurements of the same sample is

590 depicted (black line) with the standard deviation (grey area). (C) The morphology and
591 size of EVs was observed with transmission electron microscopy. Scale bar: 100 nm.
592 (D) Cell lysate (Pellet I/II) and EVs (Pellet IV) from zebrafish embryos were
593 characterized using immunoblots with antibodies detecting GP96, TSG101, LAMP1
594 and ALIX.
595

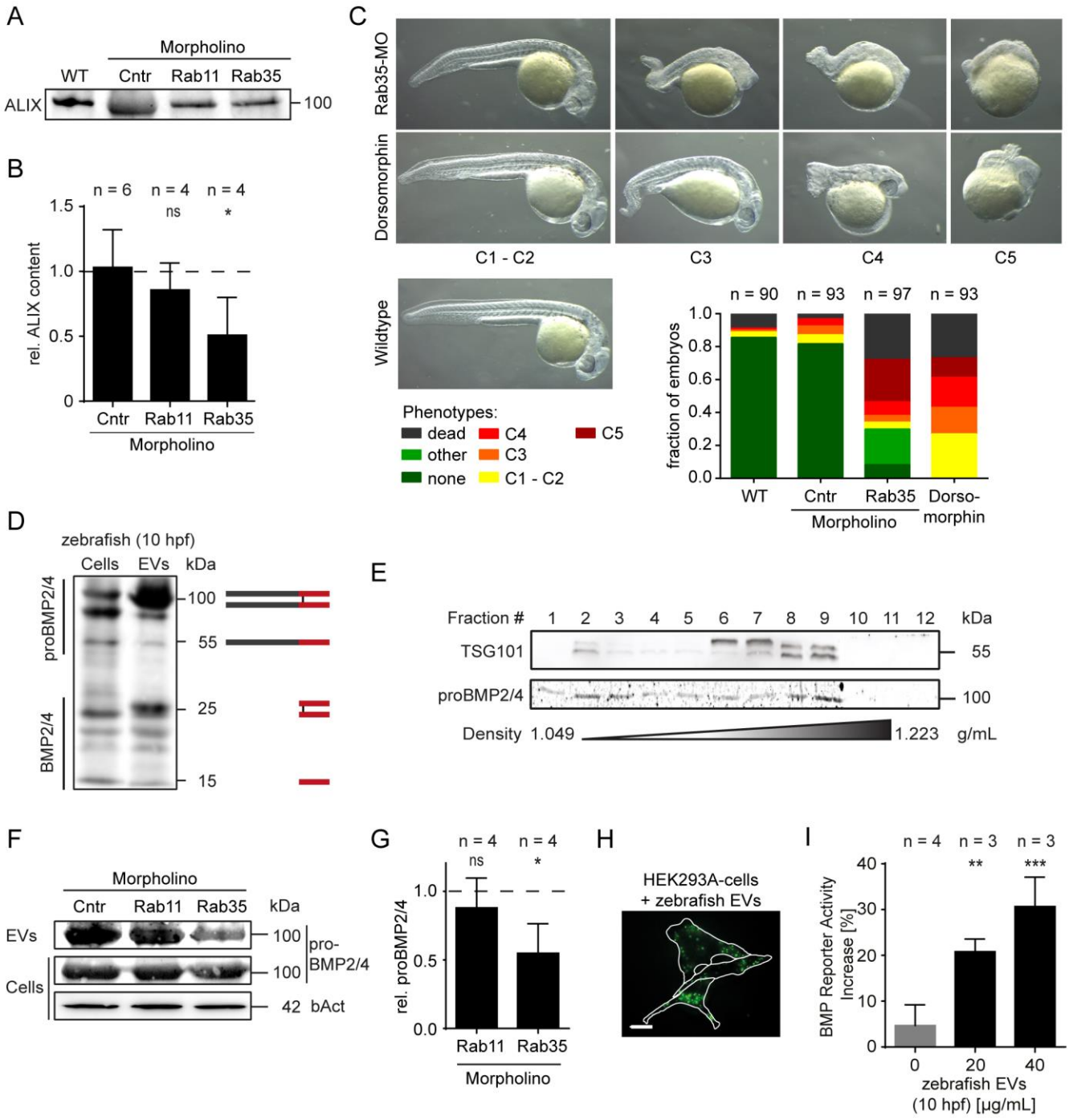

596

Figure 2 | BMP2 and/or BMP4 are transported by EVs. (A) Zebrafish embryos were injected with either 250 µM Cntr-MO, 125 µM Rab11a-MO or 250 µM Rab35-MO at the one-cell stage. EVs were isolated from these zebrafish embryos at bud stage (10 hpf). Western blot analysis with antibodies against ALIX were used to estimate the EV-content of the isolates. The quantification of the western blot signals is plotted in (B). The dashed line represents the measured signal intensity of the wildtype sample, which was used as a normalizer. The samples were compared to the Cntr-MO sample using ANOVA with Tukey's post hoc test. (C) Images of Rab35-morphants at 24 hpf displaying the spectrum of phenotype severities, resembling dorsalization. For comparison, zebrafish treated with the BMP-signalling inhibitor 10 µM dorsomorphin are shown. The embryos were classified by phenotype severity following the suggestions made by Mullins et al.[32]. The quantification of the fraction of embryos in the respective classes is plotted below the images. (D) EVs were isolated from zebrafish embryos at bud stage (10 hpf) and used in western blot experiments under non-reducing conditions to detect BMP2/4. Multiple preprocessing intermediates of BMP2/4, which are depicted schematically next to the respective protein bands, were detected (dark grey: prodomain; red: ligand domain). (E) EV isolates from zebrafish embryos were further separated on an OptiPrep™-gradient. The gradient was split into 12 fractions, which were investigated by immunoblotting with antibodies targeting TSG101 and BMP2/4. (F) Cell lysate and EVs from Cntr-, Rab11- and Rab35-morphants were investigated for differences in BMP2/4-content by western blot analysis. The quantification of BMP2/4-band intensities in EV isolates is shown in (G). The samples were compared to the normalized mean of the Cntr-morphants (dashed

620 line) using one-sample t-tests with Bonferroni correction for multiple testing. (H)
621 HEK293A-cells were treated with PKH26-labeled EVs isolated from zebrafish embryos
622 and imaged after 5 h. White lines depict cell borders. The scale bar represents 20 µm.
623 (I) HEK293A-cells transiently expressing pGL3-BRE:Luciferase and pIS2-Renilla were
624 treated with unlabelled zebrafish EVs and used in dual luciferase assay 16 h after
625 treatment. Values were normalized to an independent untreated control sample.
626 Samples were compared using ANOVA with Tukey's post hoc test.
627

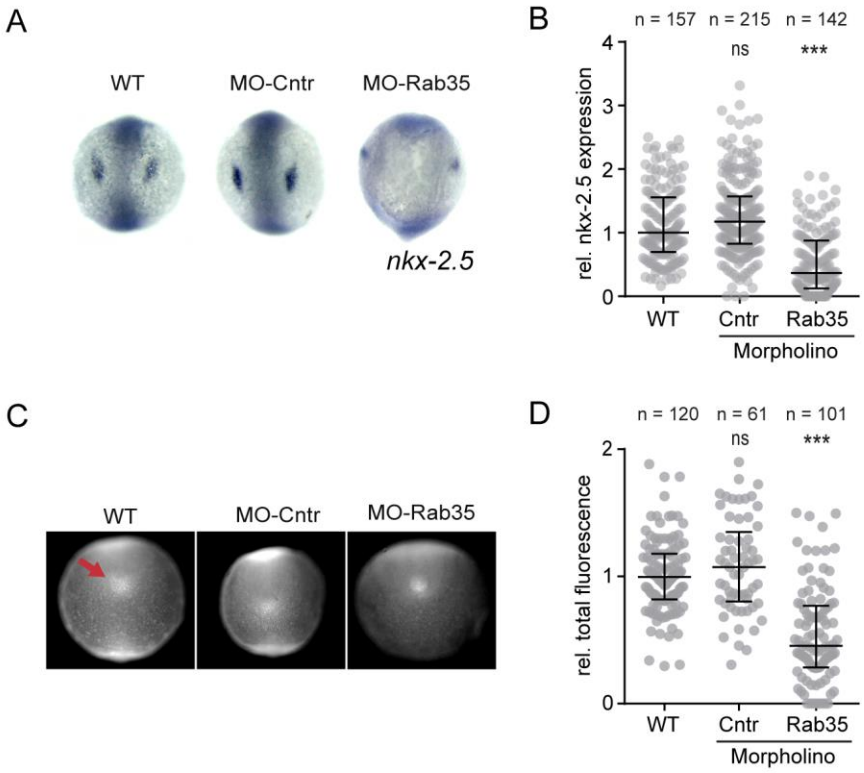

628

629 **Figure 3 | Rab35-KD reduces BMP2/4-dependent signalling activity.** Wildtype
630 zebrafish embryos, Cntr- and Rab35-morphants were collected at the 7-somite stage.
631 (A-B) Whole mount *in situ* hybridizations was performed to detect *nkx-2.5*. Image
632 analysis-based quantification was used to measure the *nkx-2.5* expression in the
633 embryos. (C) Typical whole mount immunofluorescence stainings detecting
634 phosphorylated Smad1/5/9 are shown. The tail bud is indicated by the red arrow. (D)
635 The Smad1/5/9-phosphorylation was quantified in the tail bud. The total fluorescence
636 is defined by the product of the stained area, which was normalized to the area of the
637 embryo, and the background corrected fluorescence intensity. All statistical
638 comparisons were performed by using the Kruskal-Wallis-Test with Dunn's post hoc
639 test. In the plots (C, D) the middle lines represent the median and whiskers represent
640 the 25 % and 75 %-quantiles.

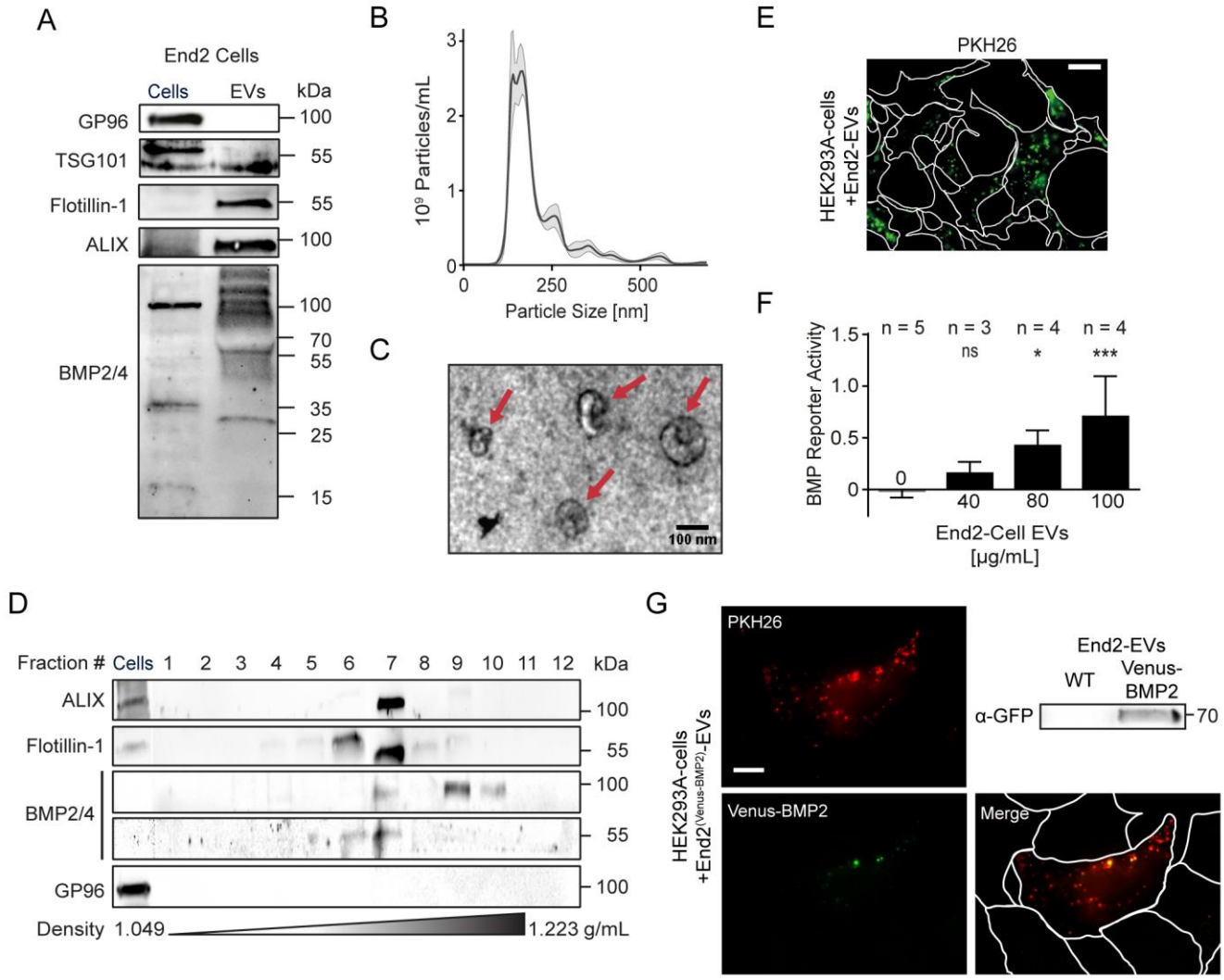

641

642 **Figure 4 | The endoderm is a source for EV-associated BMP2/4.** EVs were isolated
643 from End2-cells following the protocol described by Gross et al.[14]. (A) Western blot
644 analysis of End2 cell lysates and End2 EVs using antibodies targeting GP96, TSG101,
645 Flotillin-1, ALIX and BMP2/4. (B) NTA-measurement of a representative End2 EV-
646 isolate. The black line represents the mean of five consecutive measurements. The
647 grey area depicts the standard deviation of these measurements. (C) Representative
648 electron microscopy image of End2-EVs. Red arrows mark exosome-sized EVs. The
649 scale bar represents 100 nm. (D) OptiPrep™-gradient centrifugation was performed

650 on End2-EV isolates. Gradients were separated into 12 fractions and analysed by
651 western blotting. (E) HEK293A-cells were treated with PKH26-labeled End2-EVs for 5 h
652 before life-cell imaging. The scale represents 20 µm. White lines represent cell
653 borders. (F) HEK293A-cells transfected with pGL3-BRE:Luciferase and pIS2-Renilla
654 were treated with End2-EVs for 16 h. BMP-signalling activity was measured using a
655 dual luciferase assay. Values were normalized to an independent untreated control
656 sample. Samples were compared using ANOVA with Tukey's post hoc test. (G) EVs
657 were isolated from End2-cells transfected with a plasmid encoding Venus-BMP.
658 Western blotting was used to show the presence of Venus-BMP in EV-isolates.
659 HEK293A-cells treated with PKH26-labeled End2$^{\text{Venus BMP}}$-EVs for 5 h. The scale bar
660 represents 20 µm. The white lines represent cell borders. Merged image shows co-
661 localization of Venus-BMP and PKH26, indicating association of BMP with EVs.
662

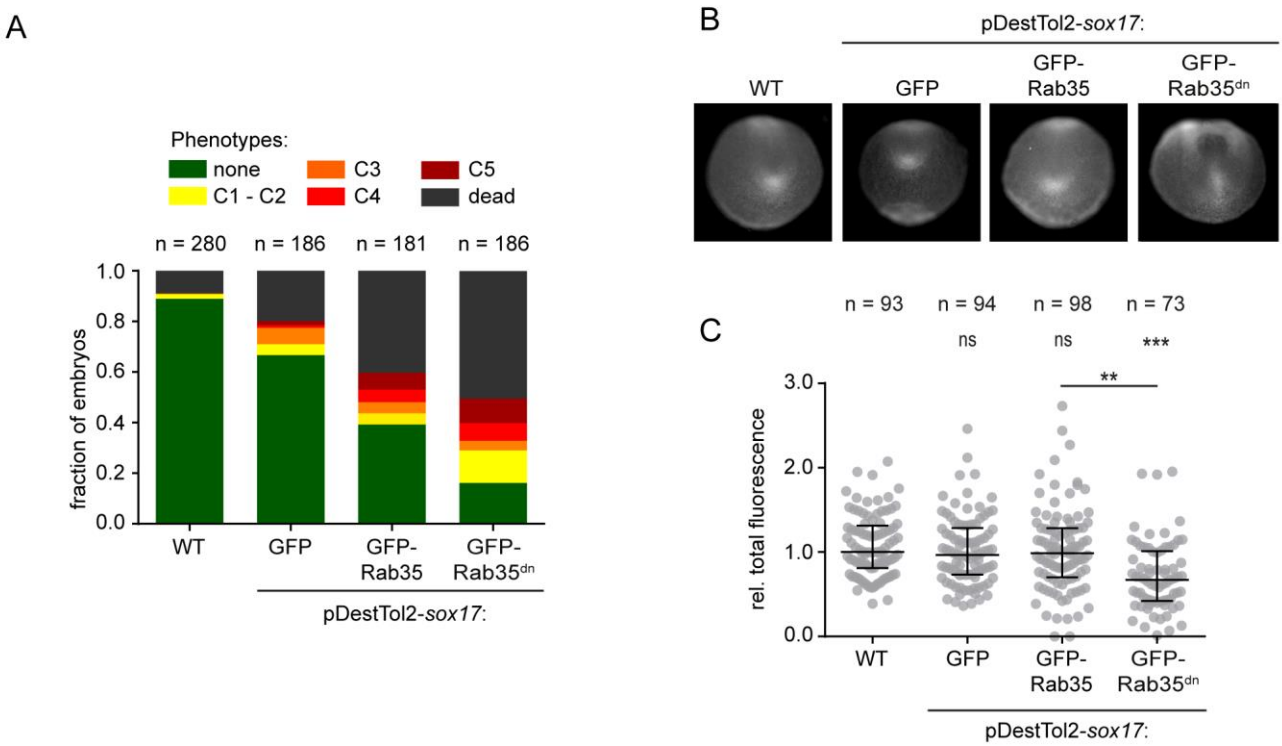

663

664 **Figure 5 | EV-secretion from the endoderm is needed for BMP-signalling during early**
665 **development.** Zebrafish embryos were injected with a pDestTol2 vector encoding
666 either GFP, GFP-Rab35 or the dominant negative GFP-Rab35$^{N120I\ (dn)}$ under the
667 transcriptional control of the *sox17*-promoter. (A) Phenotypes were assessed at
668 24 hpf. (B) Whole mount immunofluorescence stainings were used to label
669 pSmad1/5/9. Embryos were imaged in the posterior view. (C) The pSmad1/5/9
670 labelling intensity in the tail bud was quantified. The distributions were compared
671 using the Kruskal-Wallis-test in combination with Dunn's post hoc test.

672

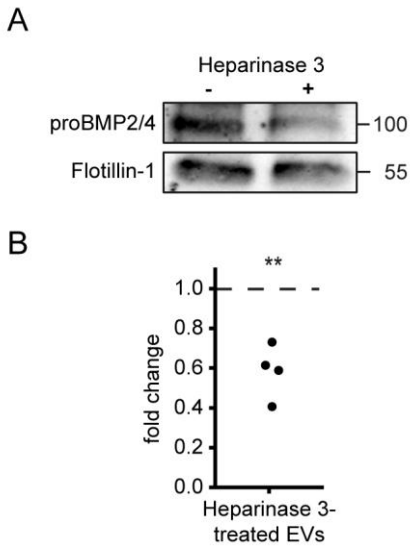

673

674 **Figure 6 | BMP2/4 is tethered to EV-surfaces by binding to HSPGs.** End2-EV isolates
675 were split into two equal fractions and either treated with Heparinase 3 or with
676 Heparinase 3 reaction buffer. (A) Representative immunoblot of Heparinase 3-treated
677 and control EV-samples. (B) proBMP2/4-band intensities were normalized with the
678 respective Flotillin-1-band intensities. The Heparinase 3-treated sample was further
679 normalized to the control and a one-sample t-test was used to determine whether the
680 amount of proBMP2/4 in EVs was significantly reduced after Heparinase 3-treatment.

681

Supplementary Information

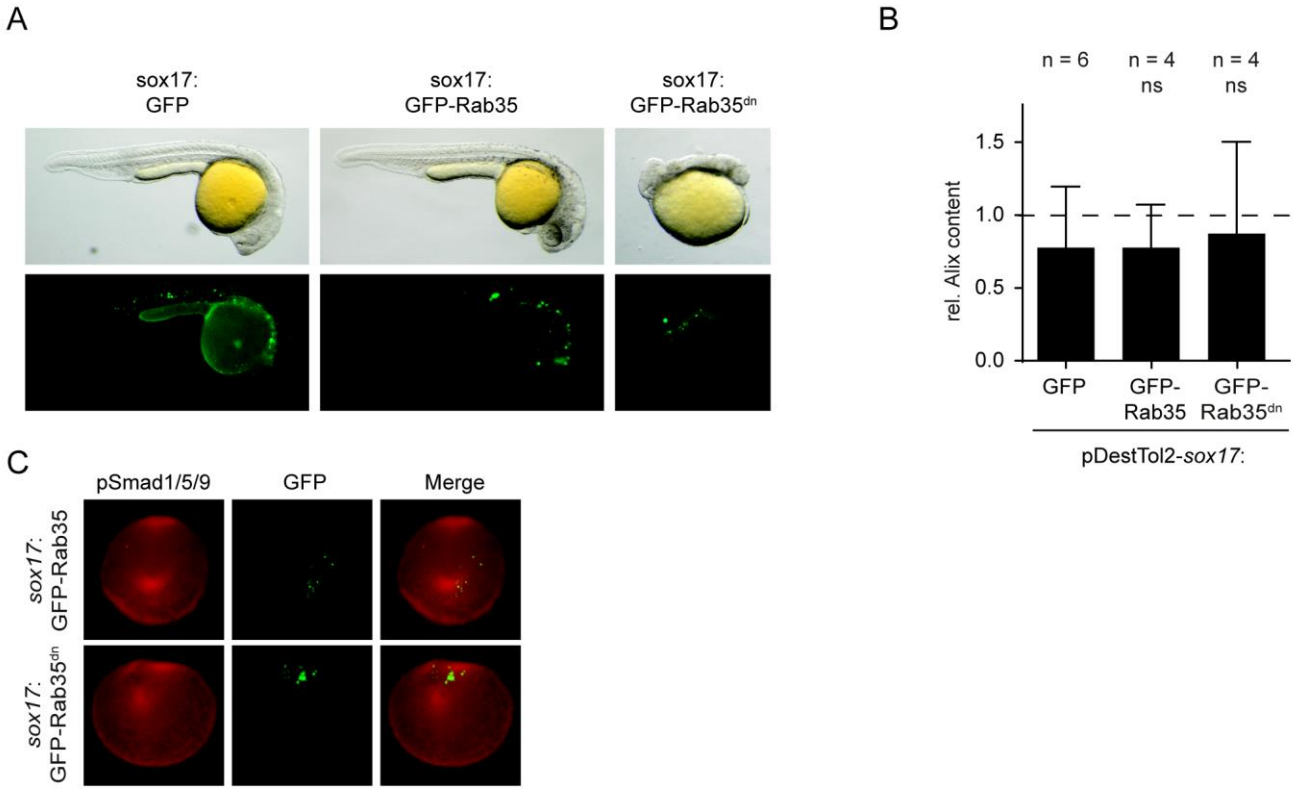

Figure S1 | Mosaic expression of dominant negative Rab35 in the endoderm does not result in a measurable reduction in secreted EVs. (A) Images of zebrafish embryos at 24 hpf expressing either pDestTol2-*sox17*:GFP, pDestTol2-*sox17*:GFP-Rab35, pDestTol2-*sox17*:GFP-Rab35^{dn}. (B) The amount of secreted EVs in transgene-expressing zebrafish was measured by determining the ALIX-content in EV-isolates of 10 hpf-zebrafish embryos using western blotting. The values were normalized to the wildtype-control and the means were compared using ANOVA and Tukey's post hoc test. (C) Representative images showing the merge of the GFP-fluorescence representing the transgene and pSmad1/5/9-immuno fluorescence staining.

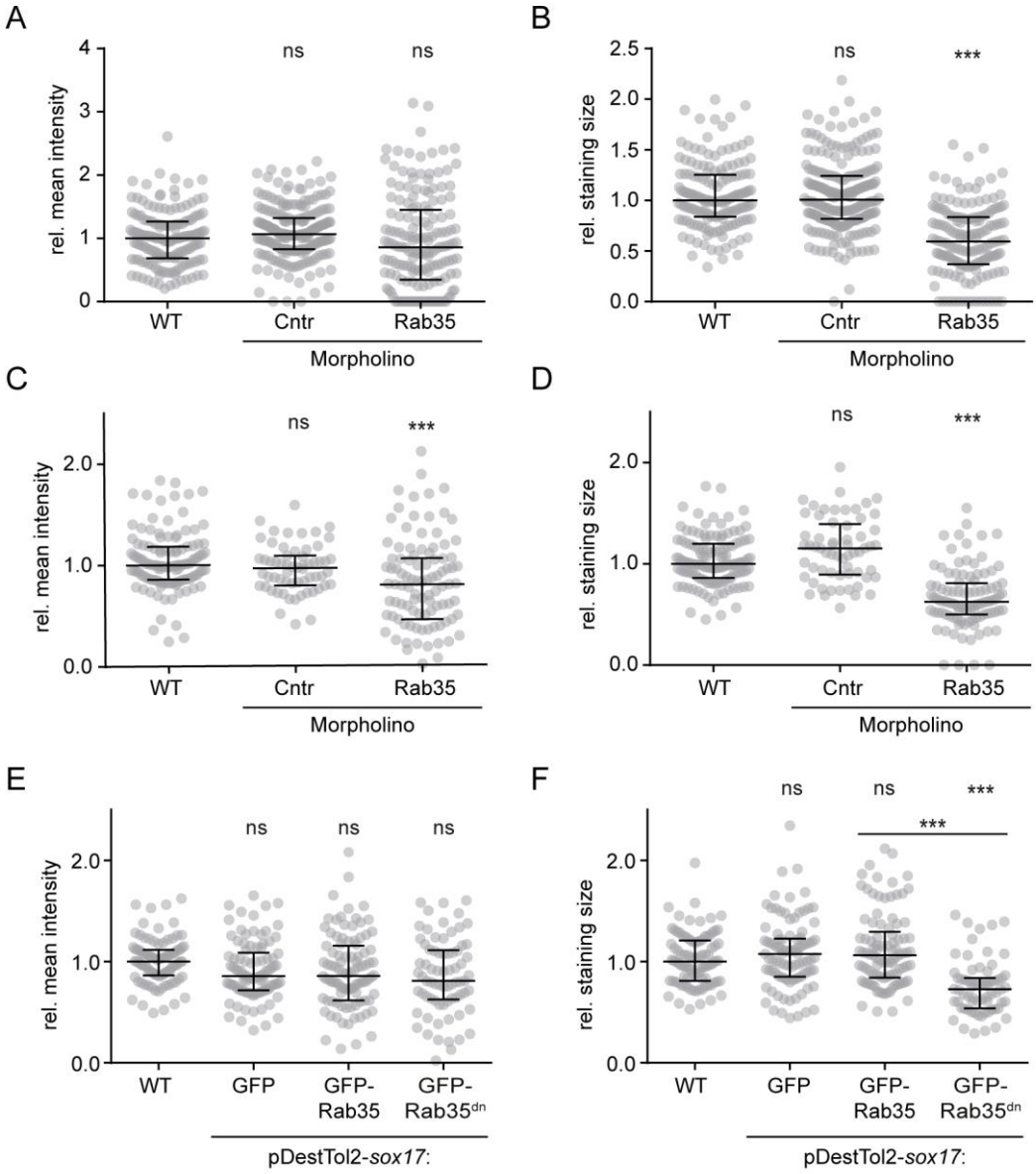

694

695 **Figure S2 | The staining area is the predominant factor determining the reduced *in***

696 ***vivo* BMP-signalling response after Inhibition of EV-secretion.** Scatter-whisker-charts

697 plotting the parameters used to calculate the *nkx2.5*-expression A, B; Figure 3B) and

698 total fluorescence in the tail buds of pSmad1/5/9 immunofluorescence stainings (C,

699 D; Figure 3D) in Rab35-morphants as well as the total fluorescence in pSmad1/5/9-

700 immunofluorescence stainings of zebrafish embryos expressing GFP-Rab35^{dn} in the

701 endoderm (E, F; Figure 5D). (A, C, E) The background-corrected mean intensity
702 measured in the labelled regions of interest. (B, D, F) The area of the regions of interest
703 normalized with the area of the embryo. Sample distributions were compared using
704 the Kruskal-Wallis-test with Dunn's post hoc test.